

1

2

Regulation of midgut cell proliferation impacts *Aedes aegypti*

3

susceptibility to dengue virus

4

5 Mabel L. Taracena^{1, 2}, Vanessa Bottino-Rojas^{1, 2}, Octavio A.C. Talyuli^{1, 2}, Ana Beatriz Walter-

6 Nuno^{1, 2}, José Henrique M. Oliveira^{2, 3}, Yesseinia I. Angleró-Rodríguez⁴, Michael B. Wells^{5,6},

7 George Dimopoulos⁴, Pedro L. Oliveira^{1,2}, Gabriela O. Paiva-Silva^{1,2*}

8 Affiliations:

9 1 Laboratório de Bioquímica de Artrópodes Hematófagos, Instituto de Bioquímica Médica

10 Leopoldo de Meis, Programa de Biologia Molecular e Biotecnologia, Universidade Federal do

11 Rio de Janeiro, Rio de Janeiro, Brasil, 21941-902, 2 Instituto Nacional de Ciência e Tecnologia

12 em Entomologia Molecular (INCT-EM), Brasil, 3 Departamento de Microbiologia, Imunologia

13 e Parasitologia. Universidade Federal de Santa Catarina. Florianópolis, SC, Brazil, 88040-970.4

14 W. Harry Feinstone Department of Molecular Microbiology and Immunology, Bloomberg

15 School of Public Health, Johns Hopkins University, Baltimore, MD 21205, USA; 5 Department

16 of Cell Biology, Johns Hopkins University School of Medicine, Baltimore, MD 21205, USA, 6

17 Johns Hopkins Malaria Research Institute, Johns Hopkins Bloomberg School of Public Health,

18 Baltimore, MD 21205, USA.

19 (*) Corresponding author

20 E-mail: gosilva@bioqmed.ufrj.br

21

22 Keywords: *Aedes aegypti*, Intestinal Stem Cell, Dengue virus, viral infection, midgut

23 homeostasis, strain susceptibility, RNAi, Notch ligand Delta, vector competence

24

25 **Abstract**

26 *Aedes aegypti* is the vector of some of the most important vector-borne diseases like
27 Dengue, Chikungunya, Zika and Yellow fever, affecting millions of people worldwide. The
28 cellular processes that follow a blood meal in the mosquito midgut are directly associated with
29 pathogen transmission. We studied the homeostatic response of the midgut against oxidative
30 stress, as well as bacterial and dengue virus (DENV) infections, focusing on the proliferative
31 ability of the intestinal stem cells (ISC). Inhibition of the peritrophic matrix (PM) formation led
32 to an increase in ROS production by the epithelial cells in response to contact with the resident
33 microbiota, suggesting that maintenance of low levels of ROS in the intestinal lumen is key to
34 keep ISCs division in balance. We show that dengue virus infection induces midgut cell division
35 in both DENV susceptible (Rockefeller) and refractory (Orlando) mosquito strains. However,
36 the susceptible strain delays the activation of the regeneration process compared with the
37 refractory strain. Impairment of the Delta/Notch signaling, by silencing the Notch ligand Delta
38 using RNAi, significantly increased the susceptibility of the refractory strains to DENV
39 infection of the midgut. We propose that this cell replenishment is essential to control viral
40 infection in the mosquito. Our study demonstrates that the intestinal epithelium of the blood fed
41 mosquito is able to respond and defend against different challenges, including virus infection. In
42 addition, we provide unprecedented evidence that the activation of a cellular regenerative
43 program in the midgut is important for the determination of the mosquito vectorial competence.

44

45

46

47

48

49

50 **Authors' summary**

51 *Aedes* mosquitoes are important vectors of arboviruses, representing a major threat to public
52 health. While feeding on blood, mosquitoes address the challenges of digestion and preservation
53 of midgut homeostasis. Damaged or senescent cells must be constantly replaced by new cells to
54 maintain midgut epithelial integrity. In this study, we show that the intestinal stem cells (ISCs)
55 of blood-fed mosquitoes are able to respond to abiotic and biotic challenges. Exposing midgut
56 cells to different types of stress, such as the inhibition of the peritrophic matrix formation,
57 changes in the midgut redox state, or infection with entomopathogenic bacteria or viruses,
58 resulted in an increased number of mitotic cells in blood-fed mosquitoes. Mosquito strains with
59 different susceptibilities to DENV infection presented different time course of cell regeneration
60 in response to viral infection. Knockdown of the Notch pathway in a refractory mosquito strain
61 limited cell division after infection with DENV and resulted in increased mosquito
62 susceptibility to the virus. Conversely, inducing midgut cell proliferation made a susceptible
63 strain more resistant to viral infection. Therefore, the effectiveness of midgut cellular renewal
64 during viral infection proved to be an important factor in vector competence. These findings can
65 contribute to the understanding of virus-host interactions and help to develop more successful
66 strategies of vector control.

67

68

69

70

71

72

73

74

75 **Introduction**

76 The mosquito *Aedes aegypti* is a vector of several human pathogens, such as flaviviruses,
77 including Yellow fever (YFV), Dengue (DENV) and Zika (ZIKV), and thus this mosquito
78 exerts an enormous public health burden worldwide [1,2]. During the transmission cycle, these
79 insects feed on volumes of blood that are 2-3 times their weight, and the digestion of this large
80 meal results in several potentially damaging conditions [3]. The digestion of blood meal
81 requires intense proteolytic activity in the midgut and results in the formation of potentially
82 toxic concentrations of heme, iron, amino acids and ammonia [4]. The midgut is also the first
83 site of interaction with potential pathogens, including viruses, and supports a dramatic increase
84 in intestinal microbiota after blood feeding [5,6]. To overcome these challenges, the ingestion of
85 a blood meal is followed by several physiological processes, such as formation of a peritrophic
86 matrix (PM) [7,8] and down-regulation of reactive oxygen species (ROS) production. In
87 addition, the midgut epithelium is the first barrier that viruses must cross in the mosquito to
88 achieve a successful viral cycle (reviewed in [9]). Thus, in order to ensure epithelial integrity
89 and the maintenance of midgut homeostasis, the midgut epithelium must fine tune key cellular
90 mechanisms, including cell proliferation and differentiation.

91 In both vertebrate and invertebrate animals, the gut epithelia have a similar basic cellular
92 composition: absorptive enterocytes (ECs) that represent the majority of the differentiated cells
93 and are interspersed with hormone-producing enteroendocrine cells (ee). The intestinal stem
94 cells (ISCs) and enteroblasts (EB) account for the progenitor cells, responsible for replenishing
95 the differentiated cells that are lost due to damage or aging [10–14]. In *A. aegypti*, description of
96 the different cellular types and functions started with identification and basic characterization of
97 absorptive (ECs) and non-absorptive cells (ISC, EB, and enteroendocrine cells) [15]. To date,
98 the study of division properties of the ISCs in this vector species remains limited to the
99 description of the division process during metamorphosis [16].

100 Several conserved signaling pathways are known to be involved in midgut tissue renewal and
101 differentiation. Comparative genomic analysis of some of these pathways has been done

102 between *Drosophila melanogaster* and vector mosquitoes [17,18], but functional studies in
103 *Aedes*, under the context of tissue regeneration, are still necessary. Notably, the Notch signaling
104 pathway regulates cell differentiation in the midgut of both mammals and *Drosophila*. In
105 *Drosophila*, loss of function of Notch is attributed to the increase of intestinal cell proliferation
106 and tumor formation [19]. However, it has already been shown that depletion of Notch in
107 *Drosophila* ISCs also leads to stem cell loss and premature cell formation [20]. Accordingly,
108 disruption of Notch signaling in mice has resulted in decreased cell proliferation coupled with
109 secretory cell hyperplasia, whereas hyperactivation of Notch signaling results in expanded
110 proliferation with increased numbers of absorptive enterocytes [21], as also observed in
111 *Drosophila* [20].

112 In *Drosophila*, the ingestion of cytotoxic agents, such as dextran sodium sulfate (DSS),
113 bleomycin or paraquat, or infection by pathogenic bacteria can stimulates cell turnover,
114 increasing the midgut ISC mitotic index [18,22]. Similar to that, it has been recently shown that
115 cell damage produced by ingestion of several stressors also induced intestinal cell proliferation
116 in sugar-fed *Aedes albopictus* [23]. Likewise, viral infections can trigger cellular responses,
117 such as apoptosis or autophagy, in different infection models [24–27]. However, the interplay
118 between intestinal cell proliferation and pathogen transmission has been a neglected subject in
119 the literature.

120 In this study, we have characterized the dynamics of *A. aegypti* intestinal epithelium
121 proliferation during blood meal digestion in response to oxidative stress, bacterial infections,
122 and viral infections. We have also shown that two mosquito strains with different DENV
123 susceptibilities [28] presented differences in cell mitotic rates after viral infection. Finally, our
124 results indicate for the first time that the ability to replenish midgut cells by modulation of cell
125 renewal involves the Delta-Notch signaling and is a key factor that influences *A. aegypti*
126 competence to transmit DENV. We show that the cell proliferation rates influences mosquito
127 infection and vector competence for DENV.

128

129

130 **Results**

131 *Aedes aegypti* adult females acquire DENV and other arboviruses during the blood feedings that
132 are needed to complete the reproductive cycle of the mosquito. To characterize the epithelial
133 adaptation to this event, we first evaluated the cellular response to the blood meal itself. Upon
134 ingestion, the blood induces dramatic changes in the Red strain mosquito midgut at a chemical,
135 microbiological and physiological level. We attempted to dissect each of these challenges, to
136 understand the delicate balance of the factors that play a role in the intestinal micro-environment
137 in which the arbovirus has to thrive in order to pass to the salivary gland and be transmitted.

138 **Characterization of the adult intestinal cells and their regenerative capacity in *A.*** 139 ***aegypti* adult midgut epithelium**

140 The tissue homeostasis of the midgut depends on the ability to replenish the damaged cells, and
141 this depends on the presence of ISCs. Due to the lack of specific markers for progenitor cells for
142 *A. aegypti*, we used morphological and physiological parameters to define the presence of ISCs
143 in the adult females. Progenitor cells are well characterized for their basal positioning and being
144 diploid, different to the apical localization of differentiated cells and the polyploidy of
145 enterocytes. Both cell types were clearly distinctive, as well as the peritrophic matrix, in the
146 midgut epithelium of blood-fed adult females (**Fig 1A**). The further characterization of ISC's
147 was performed with phospho-histone 3 antibodies, to specifically mark cells undergoing
148 mitosis. In **Fig 1B**, it can be observed the two monolayers of the *A. aegypti* midgut, where ECs
149 are clearly distinguishable and the PH3+ cell is found, with nuclei corresponding to the diploid
150 size, located basally. Clearly, not every ISC present in the tissue is going to be found
151 undergoing mitosis, but the presence of PH3+ cells, undoubtedly characterizes such cells as
152 ISCs.

153 To evaluate the homeostatic cell proliferation of the *Aedes aegypti* midgut, we observed the
154 number of cells undergoing mitosis in adult females. After a blood meal, the midgut epithelium
155 showed a lower number of cells undergoing mitosis (phospho-histone 3 positive; PH3+)

156 compared with that of sugar-fed insects (**Fig 1C and D**). To test if this decrease in mitotic cells
157 was due to progenitor cell impairment, we fed insects with blood supplemented with the pro-
158 oxidant compound paraquat. The midgut epithelium responded to an oxidative challenge by
159 increasing mitosis (**Fig 1C and D**), indicating that the intestinal stem cells maintained the
160 ability to divide and replenish damage cells after an insult at blood-fed conditions.

161

162 **Peritrophic matrix reduces cell proliferation induced by microbial infection**

163 A hallmark of blood digestion is the formation of the peritrophic matrix (PM), a chitin and
164 protein-rich non-cellular layer secreted by the midgut epithelium [7,8]. The mosquito PM
165 surrounds the blood bolus, limiting a direct contact between the epithelium, the blood meal and
166 the indigenous microbiota, thereby playing a similar function as the vertebrate digestive mucous
167 layer. Ingestion of blood contaminated with bacteria allows close contact of these
168 microorganisms to the midgut epithelium before PM formation, which is completed formed
169 only a few hours (14 to 24 hours) after a blood meal [7]. In fact, oral infection with sub-lethal
170 concentrations of the non-pathogenic *Serratia marcescens* or the entomopathogenic
171 *Pseudomonas entomophila* bacteria resulted in a significant increase in mitosis of the epithelium
172 cells (**Fig 2A and B**). The increased cell turnover was also observed when heat-killed *P.*
173 *entomophila* was provided through the blood, indicating that molecules derived from these
174 entomopathogenic bacteria are sufficient to trigger the cell proliferation program, not
175 necessarily requiring tissue infection (**Fig 2B**). In this case, tissue damage may at least partially
176 be attributed to the lack of cell membrane integrity promoted by Monalysin, a pore-forming
177 protein produced by *P. entomophila* [29].

178 Supplementation of blood with diflubenzuron (DFB), a chitin synthesis inhibitor [30], leads to
179 the inhibition of PM production, exposing the gut epithelium directly to the luminal content (**S1**
180 **Fig**). Consequently, DFB administration resulted in elevated numbers of mitotic cells (**Fig 2C**).
181 The co-ingestion of antibiotics completely abolished this effect of DFB on cell proliferation (Fig

182 2C), demonstrating that in the absence of the microbiota, the lack of the peritrophic matrix did
183 not result in elevated mitosis. These results indicate that not only oral infection with pathogenic
184 bacteria, but also the proliferation of the resident microbiota (by inhibition of PM in this case),
185 in contact with the epithelium, can trigger the midgut proliferative program.

186 Exposure of *Drosophila* enterocytes to bacteria results in ROS production as a microbiota
187 control mechanism. However, the oxidative species produced as a result of bacterial presence
188 can also cause damage to the midgut cells [31–34]. When mosquitoes were fed with blood
189 supplemented with DFB together with the antioxidant ascorbate (ASC), the mitosis levels
190 dropped significantly (**Fig 2C**). The ROS production by the midgut epithelium was assessed by
191 fluorescence microscopy using the fluorescent oxidant-sensing probe dihydroethidium (DHE).
192 As shown in **Figures 2D and E**, the midguts of DFB-fed mosquitoes exhibited a high
193 fluorescence signal, indicating an intense production of ROS. The intensity of the fluorescence
194 signal of the DFB-treated midguts was significantly reduced upon ascorbate supplementation of
195 the blood meal. Similarly, the suppression of microbiota with antibiotics dramatically reduced
196 ROS levels. These results suggest a mechanism linking PM impairment to ISC proliferation,
197 indicating that the direct exposure of the midgut epithelium to microbiota activates the
198 production of ROS as part of an immune response.

199

200 **Infection with Dengue virus affects midgut epithelia regeneration**

201 The role of epithelial tissue regeneration of the midgut upon viral infection has not been
202 investigated in mosquitoes. Thus, we decided to evaluate the gut regeneration pattern of two
203 mosquito strains that are known to exhibit different susceptibilities to DENV infection [28]. In
204 basal conditions, i.e. sugar fed, all the strains used in this study presented no difference in the
205 number of cells under mitosis (**S2 Fig**). However, after 24 hours of taking a non-infected blood
206 meal (day 1), the DENV refractory Orlando (Orl) strain presented a higher number of mitotic
207 cells compared with the susceptible Rockefeller (Rock) strain (**Fig 3A and B**), indicating that
208 the refractory strain is naturally more proliferative than the susceptible one under these

209 conditions. In the following days, both strains showed similar time course profiles of mitotic
210 activity. Upon ingestion of DENV-infected blood, the refractory Orlando strain showed an
211 increase of mitotic cells, peaking at the second day post blood meal (**Fig 3C**). Subsequently,
212 these midguts showed low numbers of cells in mitosis throughout the remaining course of
213 infection, reaching a similar number as non-infected midguts. In contrast, the susceptible
214 Rockefeller strain showed a delayed regenerative response, only reaching the maximum rate at
215 five days after infection (Fig 3C). These results suggest that the midgut cells of refractory
216 mosquitoes are able to respond more promptly to the early events of infection.

217 To test whether the differences in gut homeostatic responses between the two strains could be a
218 determinant of refractoriness/susceptibility, we disturbed the homeostatic condition of ISCs by
219 silencing *delta* expression. The Notch ligand Delta (Dl) is an upstream component of the Notch
220 pathway that is involved in cell division and differentiation. The *delta* gene is expressed in adult
221 ISC cells. Thus, accumulation of Delta is used as a marker of ISCs in *Drosophila* [19].
222 Furthermore, Delta expression is induced by infection in the *Drosophila* midgut [35]. The
223 efficiency and duration of Delta silencing by RNAi are shown in Figure 4A and Figure S3,
224 respectively. Silencing *delta* led to a significant reduction in mitosis in both mosquito strains
225 (**Fig 4B and C**). Interestingly, silencing of *delta* did not have an effect on infection
226 susceptibility in the Rockefeller strain (**Fig 4D**). In contrast, it significantly increased
227 susceptibility of the Orlando strain to DENV infection, as observed by the increased viral titers
228 in the *delta*-silenced refractory strain compared with the dsGFP-injected group (**Fig 4D**).
229 Conversely, when the susceptible strain was pre-treated with DSS, a known inducer of midgut
230 cell damage, and thereby ISC proliferation [18] and **Figure S4**, a significant reduction was seen
231 in both DENV infection intensity (**Fig 4E**) and prevalence (**Fig 4F**) in the midgut, compared
232 with non-treated mosquitoes. Similar results were observed when DSS-treated Rock mosquitoes
233 were infected with DENV4 isolates (**Fig. S5**). These data clearly indicate that the ability of
234 midguts to respond at the cellular level, via regeneration of epithelial cells, modulates the
235 success of viral infection of *A. aegypti*. Furthermore, these results show for the first time that the

236 mosquito processes required to replenish damaged cells and control tissue homeostasis are
237 determinants of vector competence.

238

239 **Discussion**

240 Cell renewal is known to be the basis of midgut epithelial integrity in model animals such as fly
241 and mice. Given the importance of the midgut epithelium in mosquitoes, where this tissue is
242 effectively the first barrier that arboviruses affront to complete the transmission cycle, we
243 decided to address the question of how this epithelium replenish its cells during the different
244 challenges of blood feeding and infection. Previous descriptive reports of epithelial cell
245 structure, function and midgut remodeling during metamorphosis [15,16,36] have shed some
246 light on this process in mosquitoes, suggesting that the cell types described in other organisms,
247 such as *Drosophila*, are also found in *A. aegypti*. Amongst the fully differentiated cells, the
248 enterocytes were clearly distinguishable by their large nuclei size, abundance and localization.
249 However, due to the current lack of mosquito specific markers for other differentiated and
250 progenitor cells, like ee's and EB's, these cells were not properly identified in mosquitoes.
251 Nonetheless, ISC hallmark capacity is to undergo mitosis, which can be marked using
252 antibodies for phosphorylated histone 3. This allowed us to successfully identify the presence of
253 ISC in the epithelium, and to quantify the number of cells dividing in the different conditions
254 evaluated (**Fig 1A-B**).

255 In the life history of mosquitoes, blood feeding represents a dramatic change from a sugar diet
256 to ingestion of a large protein-rich meal. This transition imposes challenges to midgut
257 homeostasis that are not faced by non-hematophagous insects. Knowledge about the
258 mechanisms involved in the maintenance of midgut cellular integrity and homeostasis upon
259 blood feeding or stress conditions is limited not only for *A. aegypti*, but also for other important
260 vectors. In this study, we show unique properties of the mosquito midgut, suggesting that the
261 regulation of epithelial cell proliferation is tightly regulated to allow proper handling of both

262 chemical and biological sources of stress, including DENV infection, that occur during and after
263 blood digestion. Based on these findings, we suggest that this regulation of midgut homeostasis
264 is an important determinant of viral infection dynamics in the vector gut.

265 The maximal digestion rate is attained 24 hours after a blood meal [37]. Despite the dramatic
266 increase of the microbiota, approximately 1000 times the levels before a meal [5], mosquitoes
267 seem to maintain midgut epithelial cell turnover controlled (**Fig 1C and D**). One explanation for
268 this is the physical separation between the bolus and the epithelium by the PM, as in
269 *Drosophila*. The PM is a thick extracellular layer composed mostly of chitin fibrils and
270 glycoproteins that is gradually formed after a blood meal and surrounds the blood bolus,
271 creating a physical separation from the midgut epithelium [7,8]. To preserve homeostasis, the
272 PM establishes a selective barrier, permeable to nutrients and digestive enzymes but acting as a
273 first line of defense against harmful agents. We show here that when the midgut epithelium was
274 exposed to pathogenic bacteria ingested with the blood meal, thus before PM formation, there
275 was a marked increase of mitosis (**Fig 2B**). More importantly, inhibition of the PM formation
276 also resulted in elevated mitotic cell counts (**Fig 2C**). Treating insects with antibiotics abolished
277 the mitosis upregulation promoted by chitin synthesis inhibition, further demonstrating that the
278 contact of the blood bolus itself was not the determining factor to the increase mitotic cell
279 numbers, but instead, the consequent exposure of the gut epithelium to the indigenous bacterial
280 microbiota present in the lumen was the predominant event that elicited this response. In this
281 way, the compartmentalization of the bolus may allow the enterocytes to minimize their
282 exposure to deleterious agents, and it results in reduced need to shed and replenish damaged
283 cells.

284 ROS production by midgut cells represents a major innate immunity effector mechanism that is
285 involved in the control of the microbiota. However, ROS can also damage host cells, and thus, a
286 proper balance between ROS production and microbial suppression is essential for the health of
287 the host itself [31–34,38]. Here, we show that production of ROS was activated when PM
288 formation was blocked and that this effect can be prevented by antibiotics (**Fig 2D**). Therefore,

289 we propose that the signaling mechanism that leads to increased mitosis after exposure to
290 indigenous bacteria is the production of ROS by the intestinal cells, as a defensive, yet possibly
291 damaging, response (**Fig 2**).

292 The midgut epithelial cells are the first to support viral replication within the mosquito vector
293 and several studies have addressed the immune response of the mosquito to the virus.
294 Additionally, it is well-established that changes in ROS production in the midgut impact not
295 only innate immunity responses against bacteria, but can also affect the mosquito ability to
296 transmit human pathogens [5,39–42]. Despite this comprehensive knowledge about infection-
297 related processes that occur within midgut cells, little is known about the cell turnover prior to
298 and after infection. It was our intention to evaluate if this natural process of the midgut
299 epithelium was different between mosquito strains with different degrees of susceptibility to
300 DENV. Rockefeller (Rock) and Orlando (Orl) strains are susceptible and refractory strains
301 respectively; however, under normal (sugar fed) conditions, they possess similar levels of
302 mitotic cells (**S2 Fig**) Interestingly, the Orl strain possesses higher levels of mitosis than the
303 Rock strain 24 hours after the blood meal (**Fig 3A-B**). This increased number of mitotic cells, is
304 restricted to this specific time window, as 48 hours after the feeding, the numbers are no longer
305 significantly different. This fact becomes relevant when the timeline is superposed to the
306 timeline of the initial viral infection [43]. This becomes more apparent, when the numbers of
307 mitotic cells on the susceptible Rock strain increase after 5 days, in a consistent timeline to the
308 establishment of a successful infection with higher levels of infected cells, which is not
309 observed in Orl strain that constrains the infection. In day 7, when the viruses normally leave
310 the midgut to infect other tissues [43], the mitotic rate is reduced to levels compared of non-
311 infected sugar-fed midguts (Fig 3C). Transcriptomic analyses of mosquito strains with different
312 degrees of susceptibility to DENV revealed that some genes associated with cellular
313 proliferation, growth and death are differentially expressed in refractory strains, upon DENV
314 infection [44–47]. However, this has not been directly associated to midgut regeneration in
315 these studies. In addition, the increased expression and activation of a variety of apoptotic

316 cascade components in the midgut after viral infections implicate apoptosis as part of the *A.*
317 *aegypti* defense against arboviruses [24,25,27]. Altogether, these studies pointed to the
318 significant importance of cell replenishing in the midgut epithelium to vector competence.
319 Because of that, we decided to target the Notch pathway through RNAi; to disturb the normal
320 regenerative process of the epithelium. Amongst the proteins involved in this pathway, the
321 ligand Delta was an excellent candidate for RNAi because it is upstream of the Notch signaling
322 pathway and is considered a marker of ISC [19]. Induction of RNAi by injection of dsDelta in
323 adult females, resulted in the silencing of the Notch ligand *Delta*, interrupted the normal cycle
324 of cell replenishment resulted on reduced cell division (**Fig 4B and C**), as previously reported
325 by Guo and Ohlstein (2015) in *Drosophila* and by VanDussen et al, 2012, in mice. As
326 knockdown of Delta resulted on increased DENV2 viral titers in refractory strain (**Fig 4D**), this
327 suggested that cell regeneration is also a contributing factor to the modulation of viral infection
328 and consequently to refractoriness. In addition to this result, we pre-treated mosquitoes of the
329 susceptible strain (Rockefeller) with DSS, to induce cell division. Likewise, we found that the
330 increase in mitosis was able to expand refractoriness of these mosquitoes. Our data shows for
331 the first time that the ability to replenish the epithelial differentiated cells, by ISC engagement
332 in tissue regeneration, is an important aspect of the mosquito's antiviral response in these
333 strains. Furthermore, these results revealed that the involvement of the Notch signaling pathway
334 in midgut cell proliferation is also conserved in *A. aegypti*. Additional work is required to detail
335 the mechanism by which Delta-Notch signaling interferes in midgut cell proliferation in the
336 midgut of *A. aegypti*. The role of other pathways previously shown to regulate progenitor cell
337 proliferation and differentiation in *Drosophila* and mammals, such as the Hippo, JAK-STAT
338 and other pathways, may also reveal key connections between intestinal cell replenishment and
339 vectorial competence.

340 The first 24–48 h after ingestion of virus infected blood are considered the most critical for
341 determining vector competence of a given mosquito (reviewed in [48]). Accordingly, we
342 propose that the mitotic events in the early stages of infection (e.g., 24 h after viral ingestion)

343 occur when the number of infected cells is still low and the capacity to eliminate damaged cells
344 prevents viral spreading, and therefore must be effective to limit the infection. The number of
345 mitotic cells of the refractory strain midgut at this initial time point is higher than in the
346 susceptible strain, implicating this as a likely determinant for refractoriness (**Fig 4A and B**).
347 The differences observed in the total number of mitotic cells and in the pattern of recovery
348 between Rockefeller and Orlando strains may suggest more extensive damage in the midgut of
349 the susceptible mosquitoes caused by virus infection. However, the correlation between viral
350 infection progression, cell damage and regenerative responses in the early infection remains to
351 be investigated.

352 In conclusion, our data suggest that the midgut infection by DENV is favored by delayed
353 midgut renewal in a permissive mosquito strain and that refractoriness would be supported, at
354 least partly, by the capacity to promptly activate the ISC division program. At the present time,
355 Dengue, Chikungunya and Zika viruses are widespread across the globe, and the understanding
356 of the multiple factors affecting virus infection within the mosquito is crucial. The fact that
357 faster cell renewal could be related to refractoriness adds up a new factor to be considered
358 among the many determinants of vector competence and opens up the spectrum of the vector
359 physiological events that are important when studying viral transmission. Future research is
360 required to test if other DENV refractory field strains also possess differential tissue
361 homeostatic properties and if a similar mechanism will occur in other arboviral infections.
362 These findings reveal a new path towards a better understanding of vector competence, and may
363 support the development of alternative strategies of virus transmission control.

364 Finally, these results highlight that the rate of midgut cell renewal should be taken into account
365 when choosing mosquito strains for vector control strategies that use population replacement,
366 such as SIT or *Wolbachia* based methodologies.

367

368

369

370 **Materials and Methods**

371 **Ethics statement**

372 All experimental protocols and animal care were carried out in accordance to the institutional
373 care and use committee (Comitê para Experimentação e Uso de Animais da Universidade
374 Federal do Rio de Janeiro/CEUA-UFRJ) and the NIH Guide for the Care and Use of Laboratory
375 Animals (ISBN 0–309-05377-3). The protocols were approved under the registry CEUA-UFRJ
376 #155/13. All animal work at JHU was conducted in strict accordance with the recommendations
377 in the Guide for the Care and Use of Laboratory Animals of the National Institutes of Health
378 (NIH), USA. The protocols and procedures used in this study were approved by the Animal
379 Care and Use Committee of the Johns Hopkins University (Permit Number: M006H300) and
380 the Johns Hopkins School of Public Health Ethics Committee.

381

382 **Rearing of *A. aegypti* mosquitoes**

383 The *Aedes aegypti* (Red Eye strain) were raised at the insectary of UFRJ under a 12-hour
384 light/dark cycle at 28°C and 70–80% relative humidity. The adults were maintained in a cage
385 and given a solution of 10% sucrose *ad libitum* unless specified otherwise. The *Aedes aegypti*
386 (Rockefeller and Orlando strains) were raised at the insectary of JHU under a 12-hourlight/dark
387 cycle, at 27°C and 95% humidity. The adults were maintained in a cage and given a solution of
388 10% sucrose *ad libitum*. The adult females were dissected at different times after blood feeding
389 for the experiments.

390

391 **Mosquito antibiotic treatment**

392 The mosquitoes were rendered free of cultivable bacteria by maintaining them on a 10% sucrose
393 solution with penicillin (100 u/mL), and, streptomycin (100 µg/mL) from the first day post-
394 eclosion until the time of dissection post blood feeding.

395 **Mosquito meals**

396 The *Aedes aegypti* mosquitoes from the Red Eye strain (four- to seven-days-old) were
397 artificially fed with heparinized rabbit blood. The feeding was performed using water-jacketed
398 artificial feeders maintained at 37°C and sealed with parafilm membranes. The insects were
399 starved for 4-8 hours prior to the feeding. Unfed mosquitoes were removed from the cages in all
400 the experiments.

401 The oxidative challenge was provided by addition of 500 µM of paraquat (ChemService, West
402 Chester, PA, USA) to the blood meal. As an antioxidant treatment, 50mM of ascorbic acid
403 (neutralized to pH 7.0 with NaOH) was also added to blood. The mosquitoes were orally
404 infected by *Serratia marcescens* BS 303 strain or *Pseudomonas entomophila* L48 strain at a
405 concentration of 10⁵ bacteria/mL of blood. Briefly, overnight cultures were used either live or
406 after heat inactivation. Inactivation of *P. entomophila* was done by heating at 98°C for 1 hour.
407 Live and heat-killed bacteria were all pelleted after OD600 measurements to achieve final
408 concentration of 10⁵ bacteria/mL of blood. The media supernatant was discarded and the cell
409 pellet was resuspended in blood previous to the mosquito feeding. The compound diflubenzuron
410 (DFB) (0.4 g/L), a well-known chitin synthesis inhibitor, was added to the blood meal to
411 prevent the peritrophic matrix establishment [30].

412 To stimulate ISC proliferation and midgut regeneration [18], the mosquitoes were fed with 1%
413 DSS (dextran sulfate sodium salt 6.5-10 kDa, Sigma, St. Louis, MO, USA) dissolved in 10%
414 sucrose for 2 days before infection. Twelve hours prior to infection, the DSS-sucrose solution
415 was substituted with a 10% sucrose solution to remove residual DSS from the midgut content.
416 The control mosquitoes were fed with 10% sucrose only. The infection with DENV was carried
417 out as described in the following sections.

418

419

420

421 **Proliferation and mitotic cells quantification**

422 The quantification of mitosis in whole midgut tissues was performed by PH3 labeling as
423 described elsewhere [49]. Briefly, female adult mosquitoes were dissected in PBS. Midguts
424 were fixed in PBS with 4% paraformaldehyde for 30 minutes at room temperature. Samples
425 were washed in PBS for 2 times of 10 minutes each. Then the tissues were permeabilized in
426 PBS with 0.1% X-100 (for 15 min at room temperature) and blocked in a blocking solution
427 containing PBS, 0.1% Tween 20, 2.5% BSA and 10% normal goat serum for at least 30 min at
428 room temperature. All samples were incubated with primary antibody mouse anti-PH3 (1:500,
429 Merck Millipore, Darmstadt, Germany). After washing 3 times of 20 minutes each in washing
430 solution (PBS, 0.1% Tween 20, 0.25% BSA), samples were incubated with secondary goat anti-
431 mouse antibody conjugated with Alexa Fluor 488 or 546 (Thermo Fisher Scientific, MA, USA)
432 for at least 1 hour at room temperature at a dilution of 1:2000. DNA was visualized with DAPI
433 (1mg/ml, Sigma), diluted 1:1000. The gut images were acquired in a Zeiss Observer Z1 with a
434 Zeiss Axio Cam MrM Zeiss, and the data were analyzed using the AxioVision version 4.8
435 software (Carl Zeiss AG, Germany). Representative images were acquired using a Leica SP5
436 confocal laser-scanning inverted microscope with a 20X objective lens. Images were processed
437 using Las X software.

438

439 **WGA and Phalloidin staining**

440 Midguts from insects that were fed on naive blood or blood with DFB were dissected 24 h after
441 feeding and fixed in 4% paraformaldehyde for 3 h. All of the midguts were kept on PBS-15% of
442 sucrose for 12 h and then in 30% sucrose for 30 h. After a 24-h infiltration in OCT, serial
443 microtome 14- μ m-thick transverse sections were obtained and collected on slides that were
444 subsequently labeled with the lectin WGA (Wheat Germ Agglutinin; a lectin that is highly
445 specific for N-acetylglucosamine polymers) coupled to fluorescein isothiocyanate (FITC). The
446 slides were washed 3 times in PBS buffer containing 2 mg/mL BSA (PBSB). The samples were

447 then incubated in 50mM NH₄Cl/PBS for 30 min; in 3% BSA, 0.3% Triton X-100 PBS for 1 h;
448 and in PBSB solution with 100 mg/mL WGA-FITC (EY Laboratories) for 40 min. The slides
449 were then washed three times with PBSB and mounted with Vectrashield with DAPI mounting
450 medium (Vector laboratories). The sections were acquired in an Olympus IX81 microscope and
451 a CellR MT20E Imaging Station equipped with an IX2-UCB controller and an ORCAR2
452 C10600 CCD camera (Hamamatsu). Image processing was performed with the Xcellence RT
453 version 1.2 Software.

454 Midguts from insects that were fed on blood alone or blood with DENV-2 were dissected 5 days
455 after feeding and fixed in 4% paraformaldehyde using the same protocol as for mitotic cell
456 quantification. After the secondary antibody incubation washes, 30 min incubation with
457 phalloidin 1:100 (1uL) in 98uL blocking solution, along with the DAPI (1:100) was done at
458 room temperature protected from light. Samples were washed twice, for 5 minutes (stationary,
459 room temperature, protected from light) in 0.5mL washing solution and then onto slides with
460 VectaShield. Images (z-stack of 0.7 μ m slides) were taken on a Zeiss LSM700 laser scanning
461 confocal microscope at the Department of Cell Biology at JHU with a 20X objective lens and
462 processed using Zeiss Zen Black Edition software.

463

464 **ROS detection in the midgut**

465 The mosquito midguts were dissected in PBS 24h after feeding and incubated with 50 μ M of
466 dihydroethidium (hydroethidine; DHE; Invitrogen) diluted in Leibovitz-15 media supplemented
467 with 5% fetal bovine serum for 20 min at room temperature in the dark. The incubation media
468 was gently removed and replaced with a fresh dye-free media. The midguts were positioned on
469 a glass slide, and the oxidized DHE-fluorescence was observed by a Zeiss Observer Z1 with a
470 Zeiss Axio Cam MrM Zeiss using a Zeiss-15 filter set (excitation BP 546/12; beam splitter FT
471 580; emission LP 590) (Carl Zeiss AG, Germany) [5,50].

472

473 **RNA extraction and qPCR analysis**

474 For the qPCR assays, the RNA was extracted from the midgut using TRIzol (Invitrogen, CA,
475 USA) according to the manufacturer's protocol. The complementary DNA was synthesized
476 using the High-Capacity cDNA Reverse transcription kit (Applied Biosystems, CA, USA). The
477 qPCR was performed with the StepOnePlus Real Time PCR System (Applied Biosystems, CA,
478 USA) using the Power SYBR-green PCR master MIX (Applied Biosystems, CA, USA). The
479 Comparative Ct method [51,52] was used to compare the changes in the gene expression levels.
480 The *A. aegypti* ribosomal S7 gene was used as an endogenous control [53]. The oligonucleotide
481 sequences used in the qPCR assays were S7 (AAEL009496-RA): S7_F:
482 GGGACAAATCGGCCAGGCTATC and S7_R: TCGTGGACGCTTCTGCTTGTTG; Delta
483 (AAEL011396), Delta_Fwd: AAGGCAACTGTATCGGAGCG and Delta_Rev:
484 TATGACATCGCCAAACGTGC.

485

486 **Gene silencing**

487 Two- to three-day old mosquito females (Rockefeller and Orlando) were cold anesthetized and
488 69 nL of 3 µg/µL dsRNA solution was injected into the thorax. Three days after injection, the
489 mosquitoes were infected with DENV. Mosquito midguts were collected after 24h for real time
490 PCR and after 5 days for mitosis assay or DENV infection analysis. The HiScribe T7 *in vitro*
491 transcription kit (New England Biolabs) was used to synthesize the dsRNA. The unrelated
492 dsGFP was used as a control, and the silencing efficiency was confirmed through qPCR. To
493 generate dsDelta, the following oligonucleotides (containing the T7 polymerase-binding site)
494 were used:

495 dsDelta_Fwd: GTAATACGACTCACTATAGGGAGCAAGCCTAACGAGTGCAT

496 dsDelta_Rev: GTAATACGACTCACTATAGGGTTCCTTCTCACAGTGCGTCC

497

498

499 **Dengue virus propagation and mosquito infections**

500 The DENV-2 (New Guinea C strain) was propagated for 6 days in C6/36 cells maintained in
501 complete MEM media supplemented with 10% fetal bovine serum, 1% penicillin/streptomycin,
502 1% non-essential amino acids and 1% L-glutamine. The virus titer was determined by plaque
503 assay as 10^7 PFU/mL [54]. The females were infected through a blood meal containing: one
504 volume of virus, one volume of human red blood cells (commercial human blood was
505 centrifuged and the plasma removed), 10% human serum and 10% 10 mM ATP. Unfed
506 mosquitoes were removed from the cages. The midguts were dissected at 5 days post-blood
507 meal and stored individually in DMEM at -80°C until used.

508 For DENV-4 (Boa Vista 1981 strain) propagation, the virus was cultivated 6 days in C6/36 cells
509 maintained in Leibovitz-15 media supplemented with 5% fetal bovine serum, 1% non-essential
510 amino acids, 1% penicillin/streptomycin and triptose (2.9 g/L) [55]. The virus titer was
511 determined by plaque assay as 10^7 PFU/mL. The females that were pre-treated with DSS or
512 regular sucrose (control) were infected using one volume of rabbit red blood cells and one
513 volume of DENV-4. The midguts were dissected at 7 days after infection and stored
514 individually in DMEM at -80°C until used.

515

516 **Plaque assay**

517 The plaque assay was performed as previously described [28]. The BHK-21 cells were cultured
518 in complete DMEM media, supplemented with 10% fetal bovine serum, 1%
519 penicillin/streptomycin and 1% L-glutamine. One day before the assay, the cells were plated
520 into 24 wells plates at 70-80% confluence. The midguts were homogenized using a
521 homogenizer (Bullet Blender, Next, Advance) with 0.5mm glass beads. Serial dilutions (10
522 folds) were performed, and each one was inoculated in a single well. The plates were gently
523 rocked for 15 min at RT and then incubated for 45 min at 37°C and 5% CO_2 . Finally, an overlay
524 of DMEM containing 0.8% methylcellulose and 2% FBS, was added in each well, and the
525 plates were incubated for 5 days. To fix and stain the plates, the culture media was discarded

526 and a solution of 1:1 (v:v) methanol and acetone and 1% crystal violet was used. The plaque-
527 forming units (PFU) was counted and corrected by the dilution factor.

528

529 **Statistical analysis**

530 Unpaired Student's t-tests were applied where comparisons were made between two treatments
531 or two different mosquito strains, as indicated in the figure legends. Mann-Whitney U-tests
532 were used for infection intensity and chi-square tests were performed to determine the
533 significance of infection prevalence analysis. All statistical analyses were performed using
534 GraphPad 5 Prism Software (La Jolla, United States).

535

536 **Figure Legends**

537 **Fig 1. General structure of the midgut epithelium of *Aedes aegypti* and modulation of cell**
538 **proliferation upon blood meal.**

539 The midgut epithelium from a blood-fed *A. aegypti* female was fixed in PFA, and in (A)
540 sections of 0.14 μm were stained with WGA-FITC (green), red phalloidin (red) and DAPI
541 (blue). The peritrophic matrix (PM), intestinal lumen (Lumen), polyploid enterocytes (EC) and
542 basally localized – putative proliferative cells (*) – are visible. In (B), confocal image (z-stack
543 of 0.7 μm slides (20X)) of the two monolayers of the midgut of a blood-fed female, 5 days post
544 feeding, stained with Ph3 mouse antibody (green), DAPI (blue), and phalloidin (red) – Inset
545 (2x): polyploid enterocytes (EC) are Ph3-positive ISC (ISC) are visible. (C) Mosquitoes were
546 fed on a sugar solution (10% sucrose), blood or blood supplemented with 100 μM of the pro-
547 oxidant paraquat. The insect midguts were dissected 24 hours after feeding and immunostained
548 for PH3. Representative images of mitotic (PH3-labeled) cells (red) in the epithelial midgut of
549 animals fed on sugar, blood or blood supplemented with paraquat are shown. The nuclei are
550 stained with DAPI (blue). The arrowheads indicate PH3+ cells. (D) Quantification of PH3-

551 positive cells per midgut of sugar, blood or blood plus paraquat-fed mosquitoes for sugar and
552 blood and 18 for blood-paraquat fed midguts. The medians of at least three independent
553 experiments are shown (n=40 for sugar and blood and n=18 for paraquat supplemented blood).
554 The experiments were performed on Red Eye mosquito strain. The asterisks indicate
555 significantly different values, **** P<0.0001 (Student's t-test).

556

557 **Fig 2. The peritrophic matrix shapes intestinal homeostasis by limiting contact of the gut**
558 **epithelium with the microbiota and preventing ROS production.**

559 Red strain mosquitoes were fed on normal blood or blood infected with non-pathogenic *S.*
560 *marcescens* or entomopathogenic *P. entomophila* bacteria. Another group of mosquitoes was
561 fed blood supplemented with heat-killed *P. entomophila*. The midguts were dissected 24 hours
562 after feeding and immunostained for PH3. (A) Representative images of PH3-labeled mitotic
563 cells (green) of the midgut epithelium 24 h after a naïve blood meal or blood infected with *P.*
564 *entomophila*. The nuclei are stained with DAPI (blue). The arrowheads indicate PH3+ cells.
565 Scale bar=100 µm (B) Total PH3-positive cells were quantified from the midguts of mosquitoes
566 fed on naïve and bacteria-infected blood (n=25) or heat-inactivated *P. entomophila*. (n=12). The
567 medians of three independent experiments are shown. The asterisks indicate significantly
568 different values *** P<0.001 and **** P<0.0001 (Student's t-test). (C) Inhibition of PM
569 formation results in a significant increase of progenitors cells under mitosis. The mosquitoes
570 were fed blood or blood supplemented with diflubenzuron (DFB), DFB plus an antibiotic
571 cocktail (AB) or DFB plus 50 mM ascorbate (ASC). The midguts were dissected 24 hours after
572 feeding, and the mitotic indices were quantified by counting PH3+ cells. The medians of at least
573 three independent experiments are shown (n=30). The asterisks indicate significantly different
574 values *** P<0.001 and **** P<0.0001 (Student's t-test). (D) Assessments of reactive oxygen
575 species in the midguts were conducted by incubating midguts of insects fed as in (C) with a 50
576 µM concentration of the oxidant-sensitive fluorophore DHE. (E) Quantitative analysis of the

577 fluorescence images shown in (D) were performed using ImageJ 1.45s software (n = 7 – 9
578 insects).

579

580 **Fig 3. Dengue virus infection impacts midgut homeostasis in a strain specific manner.**

581 (A) Blood feeding induces different levels of PH3 positive cells in the midgut of the susceptible
582 (Rock) and refractory (Orl) strains 24 hours after the meal. Representative images of PH3
583 labeling in both strains, 24 hours after the blood meal. The nuclei are stained with DAPI. The
584 arrowheads indicate PH3+ cells. Scale bar=100 μ m. (B) Mosquitoes from the two strains were
585 blood fed and at day zero (non blood-fed) or at different days after feeding, the midguts were
586 dissected and immunostained for PH3. The red arrows indicate the time of blood feeding and
587 the time in which the digestion is completed (after blood bolus excretion). In (C) the mosquitoes
588 were fed on DENV2-infected blood and mitotic-cell counting was performed at different days
589 after infection. The red arrow indicates the time of DENV escape from the midgut to hemocoel.
590 The medians of at least three independent experiments are shown (n=30). The asterisks indicate
591 significantly different values * P<0.05 ** P<0.01 and *** P<0.001 (Student's t-test).

592

593 **Fig 4. Interference in gut homeostatic response impacts vector competence.**

594 (A). The midguts of dsRNA-injected Rockefeller and Orlando mosquitoes were dissected 24
595 days after a blood meal for silencing quantification of Delta , the ligand of Notch. Total PH3-
596 positive cells were quantified from midguts of silenced Delta or control (GFP) mosquitoes from
597 the Rockefeller (B) or Orlando (C) strains, both 1 and 5 days after blood meal. (D) dsRNA-
598 injected mosquitoes were fed DENV2-infected blood, and 5 days after the infection, the
599 midguts were dissected for the plaque assay. (E) The susceptible (Rockefeller) mosquitoes were
600 pre-treated with the tissue-damaging dextran sulfate sodium (DSS) accordingly to material and
601 methods section. Twelve hours after the end of the DSS treatment, the mosquitoes were fed with
602 DENV-2-infected blood. After 5 days, the midguts were dissected for the plaque assay. (F) The

603 percentage of infected midguts (infection prevalence) was scored from the same set of data as in
604 (E). The medians of at least three independent experiments are shown. n=20-25 in (A),(B) and
605 (C);n=20-26 in (D) and n=40 in (E). Statistical analyzes used were: Student's t-test for (A), (B)
606 and (C); Mann-Whitney U-tests were used for infection intensity (D and E); and chi-square tests
607 were performed to determine the significance of infection prevalence analysis (F). *P<0.05, **
608 P<0.01, **** P<0.0001.

609

610 **Acknowledgments**

611 We thank all members of the Laboratory of Biochemistry of Hematophagous Arthropods,
612 especially Jaciara Loredo, Mônica Sales and S.R. Cassia for providing technical assistance. We
613 also thank Dr. Helena Araujo (ICB, UFRJ) for all the technical advice and assistance with the
614 microscopy experiments. We would like to thank the Johns Hopkins Malaria Research Institute
615 Insectary.

616

617 **Financial Disclosure**

618 This work was supported by grants from the Conselho Nacional de Desenvolvimento Científico
619 e Tecnológico (CNPq) (INCT_EM, 16/2014), Coordenação de Aperfeiçoamento de Pessoal de
620 Nível Superior (CAPES) to GOPS and PLO, and Fundação Carlos Chagas Filho de Amparo à
621 Pesquisa de Estado do Rio de Janeiro (FAPERJ)(26/010.001545/2014) and by National
622 Institutes of Health, National Institute for Allergy and Infectious Disease, R01AI101431 to GD.
623 The funders had no role in study design, data collection and analysis, decision to publish, or
624 preparation of the manuscript.

625

626

627 **References**

- 628 1. Lounibos LP. Invasions by insect vectors of human disease. *Annu Rev Entomol.*
629 2002;47: 233–66. doi:10.1146/annurev.ento.47.091201.145206
- 630 2. Patterson J, Sammon M, Garg M. Dengue, Zika and Chikungunya: Emerging
631 Arboviruses in the New World. *West J Emerg Med.* 2016;17: 671–679.
632 doi:10.5811/westjem.2016.9.30904
- 633 3. Graça-Souza A V., Maya-Monteiro C, Paiva-Silva GO, Braz GRC, Paes MC, Sorgine
634 MHF, et al. Adaptations against heme toxicity in blood-feeding arthropods. *Insect*
635 *Biochem Mol Biol.* 2006;36: 322–335. doi:10.1016/j.ibmb.2006.01.009
- 636 4. Sterkel M, Oliveira JHM, Bottino-Rojas V, Paiva-Silva GO, Oliveira PL. The Dose
637 Makes the Poison: Nutritional Overload Determines the Life Traits of Blood-Feeding
638 Arthropods. *Trends Parasitol.* 2017;xx: 1–12. doi:10.1016/j.pt.2017.04.008
- 639 5. Oliveira JHM, Gonçalves RLS, Lara FA, Dias FA, Gandara ACP, Menna-Barreto RFS,
640 et al. Blood meal-derived heme decreases ROS levels in the midgut of *Aedes aegypti* and
641 allows proliferation of intestinal microbiota. *PLoS Pathog.* 2011;7.
642 doi:10.1371/journal.ppat.1001320
- 643 6. Gusmão DS, Santos A V., Marini DC, Bacci M, Berbert-Molina MA, Lemos FJA.
644 Culture-dependent and culture-independent characterization of microorganisms
645 associated with *Aedes aegypti* (Diptera: Culicidae) (L.) and dynamics of bacterial
646 colonization in the midgut. *Acta Trop.* 2010;115: 275–281.
647 doi:10.1016/j.actatropica.2010.04.011
- 648 7. Pascoa V, Oliveira PL, Dansa-Petretski M, Silva JR, Alvarenga PH, Jacobs-Lorena M, et
649 al. *Aedes aegypti* peritrophic matrix and its interaction with heme during blood
650 digestion. *Insect Biochem Mol Biol.* 2002;32: 517–23. doi:10.1016/S0965-
651 1748(01)00130-8

- 652 8. Shao L, Devenport M, Jacobs-Lorena M. The peritrophic matrix of hematophagous
653 insects. *Arch Insect Biochem Physiol.* 2001;47: 119–125. doi:10.1002/arch.1042
- 654 9. Franz AWE, Kantor AM, Passarelli AL, Clem RJ. Tissue barriers to arbovirus infection
655 in mosquitoes. *Viruses.* 2015;7: 3741–3767. doi:10.3390/v7072795
- 656 10. Ohlstein B, Spradling A. The adult *Drosophila* posterior midgut is maintained by
657 pluripotent stem cells. *Nature.* 2006;439: 470–4. doi:10.1038/nature04333
- 658 11. Micchelli C a, Perrimon N. Evidence that stem cells reside in the adult *Drosophila*
659 midgut epithelium. *Nature.* 2006;439: 475–9. doi:10.1038/nature04371
- 660 12. Jiang H, Edgar BA. Intestinal stem cell function in *Drosophila* and mice. *Curr Opin*
661 *Genet Dev.* Elsevier Ltd; 2012;22: 354–360. doi:10.1016/j.gde.2012.04.002
- 662 13. Liu X, Hodgson JJ, Buchon N. *Drosophila* as a model for homeostatic, antibacterial, and
663 antiviral mechanisms in the gut. Kline KA, editor. *PLOS Pathog.* 2017;13: e1006277.
664 doi:10.1371/journal.ppat.1006277
- 665 14. Ayyaz A, Jasper H. Intestinal inflammation and stem cell homeostasis in aging
666 *Drosophila melanogaster*. *Front Cell Infect Microbiol.* 2013;3: 98.
667 doi:10.3389/fcimb.2013.00098
- 668 15. Brown MR, Raikhel AS, Lea AO. Ultrastructure of midgut endocrine cells in the adult
669 mosquito, *Aedes aegypti*. *Tissue Cell.* 1985;17: 709–721. doi:10.1016/0040-
670 8166(85)90006-0
- 671 16. Fernandes KM, Neves CA, Serr??o JE, Martins GF. *Aedes aegypti* midgut remodeling
672 during metamorphosis. *Parasitol Int.* Elsevier Ireland Ltd; 2014;63: 506–512.
673 doi:10.1016/j.parint.2014.01.004
- 674 17. Behura SK, Haugen M, Flannery E, Sarro J, Tessier CR, Severson DW, et al.
675 Comparative genomic analysis of *drosophila melanogaster* and vector mosquito
676 developmental genes. *PLoS One.* 2011;6. doi:10.1371/journal.pone.0021504

- 677 18. Amcheslavsky A, Jiang J, Ip YT. Tissue Damage-Induced Intestinal Stem Cell Division
678 in *Drosophila*. *Cell Stem Cell*. Elsevier Inc.; 2009;4: 49–61.
679 doi:10.1016/j.stem.2008.10.016
- 680 19. Ohlstein B, Spradling A. Multipotent *Drosophila* intestinal stem cells specify daughter
681 cell fates by differential notch signaling. *Science*. 2007;315: 988–92.
682 doi:10.1126/science.1136606
- 683 20. Guo Z, Ohlstein B. Bidirectional Notch signaling regulates *Drosophila* intestinal stem
684 cell multipotency. *Science* (80-). 2015;350: 927. doi:10.1126/science.aab0988
- 685 21. VanDussen KL, Carulli AJ, Keeley TM, Patel SR, Puthoff BJ, Magness ST, et al. Notch
686 signaling modulates proliferation and differentiation of intestinal crypt base columnar
687 stem cells. *Development*. 2012;139: 488–497. doi:10.1242/dev.070763
- 688 22. Buchon N, Broderick NA, Poidevin M, Pradervand S, Lemaitre B. *Drosophila* Intestinal
689 Response to Bacterial Infection: Activation of Host Defense and Stem Cell Proliferation.
690 *Cell Host Microbe*. Elsevier Ltd; 2009;5: 200–211. doi:10.1016/j.chom.2009.01.003
- 691 23. Janeh M, Osman D, Kambris Z. Damage-Induced Cell Regeneration in the Midgut of
692 *Aedes albopictus* Mosquitoes. *Sci Rep*. Nature Publishing Group; 2017;7: 44594.
693 doi:10.1038/srep44594
- 694 24. Ocampo CB, Caicedo PA, Jaramillo G, Ursic Bedoya R, Baron O, Serrato IM, et al.
695 Differential Expression of Apoptosis Related Genes in Selected Strains of *Aedes aegypti*
696 with Different Susceptibilities to Dengue Virus. *PLoS One*. 2013;8.
697 doi:10.1371/journal.pone.0061187
- 698 25. O’Neill K, Olson BJSC, Huang N, Unis D, Clem RJ. Rapid selection against arbovirus-
699 induced apoptosis during infection of a mosquito vector. *Proc Natl Acad Sci U S A*.
700 2015;112: E1152-61. doi:10.1073/pnas.1424469112
- 701 26. Eng MW, van Zuylen MN, Severson DW. Apoptosis-related genes control autophagy

- 702 and influence DENV-2 infection in the mosquito vector, *Aedes aegypti*. *Insect Biochem*
703 *Mol Biol*. Elsevier Ltd; 2016;76: 70–83. doi:10.1016/j.ibmb.2016.07.004
- 704 27. Clem RJ. Arboviruses and apoptosis: The role of cell death in determining vector
705 competence. *J Gen Virol*. 2016;97: 1033–1036. doi:10.1099/jgv.0.000429
- 706 28. Sim S, Jupatanakul N, Ramirez JL, Kang S, Romero-Vivas CM, Mohammed H, et al.
707 Transcriptomic Profiling of Diverse *Aedes aegypti* Strains Reveals Increased Basal-level
708 Immune Activation in Dengue Virus-refractory Populations and Identifies Novel Virus-
709 vector Molecular Interactions. *PLoS Negl Trop Dis*. 2013;7.
710 doi:10.1371/journal.pntd.0002295
- 711 29. Opota O, Vallet-Gély I, Vincentelli R, Kellenberger C, Iacovache I, Gonzalez MR, et al.
712 Monalysin, a Novel β -Pore-Forming Toxin from the *Drosophila* Pathogen *Pseudomonas*
713 *entomophila*, Contributes to Host Intestinal Damage and Lethality. *PLoS Pathog*.
714 2011;7: e1002259. doi:10.1371/journal.ppat.1002259
- 715 30. Kelkenberg M, Odman-Naresh J, Muthukrishnan S, Merzendorfer H. Chitin is a
716 necessary component to maintain the barrier function of the peritrophic matrix in the
717 insect midgut. *Insect Biochem Mol Biol*. Elsevier Ltd; 2015;56: 21–28.
718 doi:10.1016/j.ibmb.2014.11.005
- 719 31. Ha EM, Oh CT, Ryu JH, Bae YS, Kang SW, Jang I hwan, et al. An antioxidant system
720 required for host protection against gut infection in *Drosophila*. *Dev Cell*. 2005;8: 125–
721 132. doi:10.1016/j.devcel.2004.11.007
- 722 32. Ha E-M, Oh C-T, Bae YS, Lee W-J. A direct role for dual oxidase in *Drosophila* gut
723 immunity. *Science*. 2005;310: 847–50. doi:10.1126/science.1117311
- 724 33. Ha EM, Lee KA, Seo YY, Kim SH, Lim JH, Oh BH, et al. Coordination of multiple dual
725 oxidase-regulatory pathways in responses to commensal and infectious microbes in
726 *drosophila* gut. *Nat Immunol*. Nature Publishing Group; 2009;10: 949–957.

- 727 doi:10.1038/ni.1765
- 728 34. Kim S-H, Lee W-J. Role of DUOX in gut inflammation: lessons from *Drosophila* model
729 of gut-microbiota interactions. *Front Cell Infect Microbiol.* 2014;3: 1–12.
730 doi:10.3389/fcimb.2013.00116
- 731 35. Broderick NA, Buchon N, Lemaitre B. Microbiota-Induced Changes in *Drosophila*
732 melanogaster Host Gene Expression and Gut Morphology. *MBio.* 2014;5: e01117-14-
733 e01117-14. doi:10.1128/mBio.01117-14
- 734 36. Billingsley P, Lehane M. Structure and ultrastructure of the insect midgut. *Biol Insect*
735 *Midgut.* Dordrecht: Springer Netherlands; 1996; 3–30. doi:10.1007/978-94-009-1519-
736 0_1
- 737 37. Klowden MJ, Briegel H. Mosquito Gonotrophic Cycle and Multiple Feeding Potential:
738 Contrasts Between *Anopheles* and *Aedes* (Diptera: Culicidae). *J Med Entomol.* 1994;31:
739 618–622. doi:10.1093/jmedent/31.4.618
- 740 38. Bae YS, Choi MK, Lee WJ. Dual oxidase in mucosal immunity and host-microbe
741 homeostasis. *Trends Immunol.* 2010;31: 278–287. doi:10.1016/j.it.2010.05.003
- 742 39. Kumar S, Christophides GK, Cantera R, Charles B, Han YS, Meister S, et al. The role of
743 reactive oxygen species on *Plasmodium melanotic* encapsulation in *Anopheles gambiae*.
744 *Proc Natl Acad Sci U S A.* 2003;100: 14139–44. doi:10.1073/pnas.2036262100
- 745 40. Molina-Cruz A, DeJong RJ, Charles B, Gupta L, Kumar S, Jaramillo-Gutierrez G, et al.
746 Reactive Oxygen Species Modulate *Anopheles gambiae* Immunity against Bacteria and
747 *Plasmodium*. *J Biol Chem.* 2008;283: 3217–3223. doi:10.1074/jbc.M705873200
- 748 41. Ramirez JL, Souza-Neto J, Cosme RT, Rovira J, Ortiz A, Pascale JM, et al. Reciprocal
749 tripartite interactions between the *Aedes aegypti* midgut microbiota, innate immune
750 system and dengue virus influences vector competence. *PLoS Negl Trop Dis.* 2012;6: 1–
751 11. doi:10.1371/journal.pntd.0001561

- 752 42. Liu J, Liu Y, Nie K, Du S, Qiu J, Pang X, et al. Flavivirus NS1 protein in infected host
753 sera enhances viral acquisition by mosquitoes. *Nat Microbiol.* Nature Publishing Group;
754 2016;1: 16087. doi:10.1038/nmicrobiol.2016.87
- 755 43. Salazar MI, Richardson JH, Sánchez-Vargas I, Olson KE, Beaty BJ. Dengue virus type
756 2: replication and tropisms in orally infected *Aedes aegypti* mosquitoes. *BMC Microbiol.*
757 2007;7: 9. doi:10.1186/1471-2180-7-9
- 758 44. Behura SK, Gomez-Machorro C, Harker BW, deBruyn B, Lovin DD, Hemme RR, et al.
759 Global cross-talk of genes of the mosquito *Aedes aegypti* in response to dengue virus
760 infection. *PLoS Negl Trop Dis.* 2011;5. doi:10.1371/journal.pntd.0001385
- 761 45. Chauhan C, Behura SK, deBruyn B, Lovin DD, Harker BW, Gomez-Machorro C, et al.
762 Comparative Expression Profiles of Midgut Genes in Dengue Virus Refractory and
763 Susceptible *Aedes aegypti* across Critical Period for Virus Infection. *PLoS One.* 2012;7.
764 doi:10.1371/journal.pone.0047350
- 765 46. Souza-Neto JA, Sim S, Dimopoulos G. An evolutionary conserved function of the JAK-
766 STAT pathway in anti-dengue defense. *Proc Natl Acad Sci U S A.* 2009;106: 17841–6.
767 doi:10.1073/pnas.0905006106
- 768 47. Behura SK, Gomez-Machorro C, Debruyn B, Lovin DD, Harker BW, Romero-Severson
769 J, et al. Influence of mosquito genotype on transcriptional response to dengue virus
770 infection. *Funct Integr Genomics.* 2014;14: 581–589. doi:10.1007/s10142-014-0376-1
- 771 48. Severson D, Behura S. Genome Investigations of Vector Competence in *Aedes aegypti*
772 to Inform Novel Arbovirus Disease Control Approaches. *Insects.* 2016;7: 58.
773 doi:10.3390/insects7040058
- 774 49. Jin Y, Ha N, Forés M, Xiang J, Gläßer C, Maldera J, et al. EGFR/Ras Signaling Controls
775 *Drosophila* Intestinal Stem Cell Proliferation via Capicua-Regulated Genes. *PLoS Genet.*
776 2015;11: 1–27. doi:10.1371/journal.pgen.1005634

- 777 50. Kalyanaraman B, Darley-USmar V, Davies KJA, Dennery PA, Forman HJ, Grisham MB,
778 et al. Measuring reactive oxygen and nitrogen species with fluorescent probes:
779 Challenges and limitations. *Free Radic Biol Med.* Elsevier Inc.; 2012;52: 1–6.
780 doi:10.1016/j.freeradbiomed.2011.09.030
- 781 51. Schmittgen TD, Livak KJ. Analyzing real-time PCR data by the comparative CT
782 method. *Nat Protoc.* 2008;3: 1101–1108. doi:10.1038/nprot.2008.73
- 783 52. Livak KJ, Schmittgen TD. Analysis of relative gene expression data using real-time
784 quantitative PCR and the 2- $\Delta\Delta$ CT method. *Methods.* 2001;25: 402–408.
785 doi:10.1006/meth.2001.1262
- 786 53. Sim S, Dimopoulos G. Dengue virus inhibits immune responses in *Aedes aegypti* cells.
787 *PLoS One.* 2010;5. doi:10.1371/journal.pone.0010678
- 788 54. Das S, Garver L, Ramirez JR, Xi Z, Dimopoulos G. Protocol for Dengue Infections in
789 Mosquitoes (*A. aegypti*) and Infection Phenotype Determination. *J Vis Exp.* 2007; 4–5.
790 doi:10.3791/220
- 791 55. Oliveira JHM, Talyuli OAC, Gonçalves RLS, Paiva-Silva GO, Sorgine MHF, Alvarenga
792 PH, et al. Catalase protects *Aedes aegypti* from oxidative stress and increases midgut
793 infection prevalence of Dengue but not Zika. *PLoS Negl Trop Dis.* 2017;11: e0005525.
794 doi:10.1371/journal.pntd.0005525

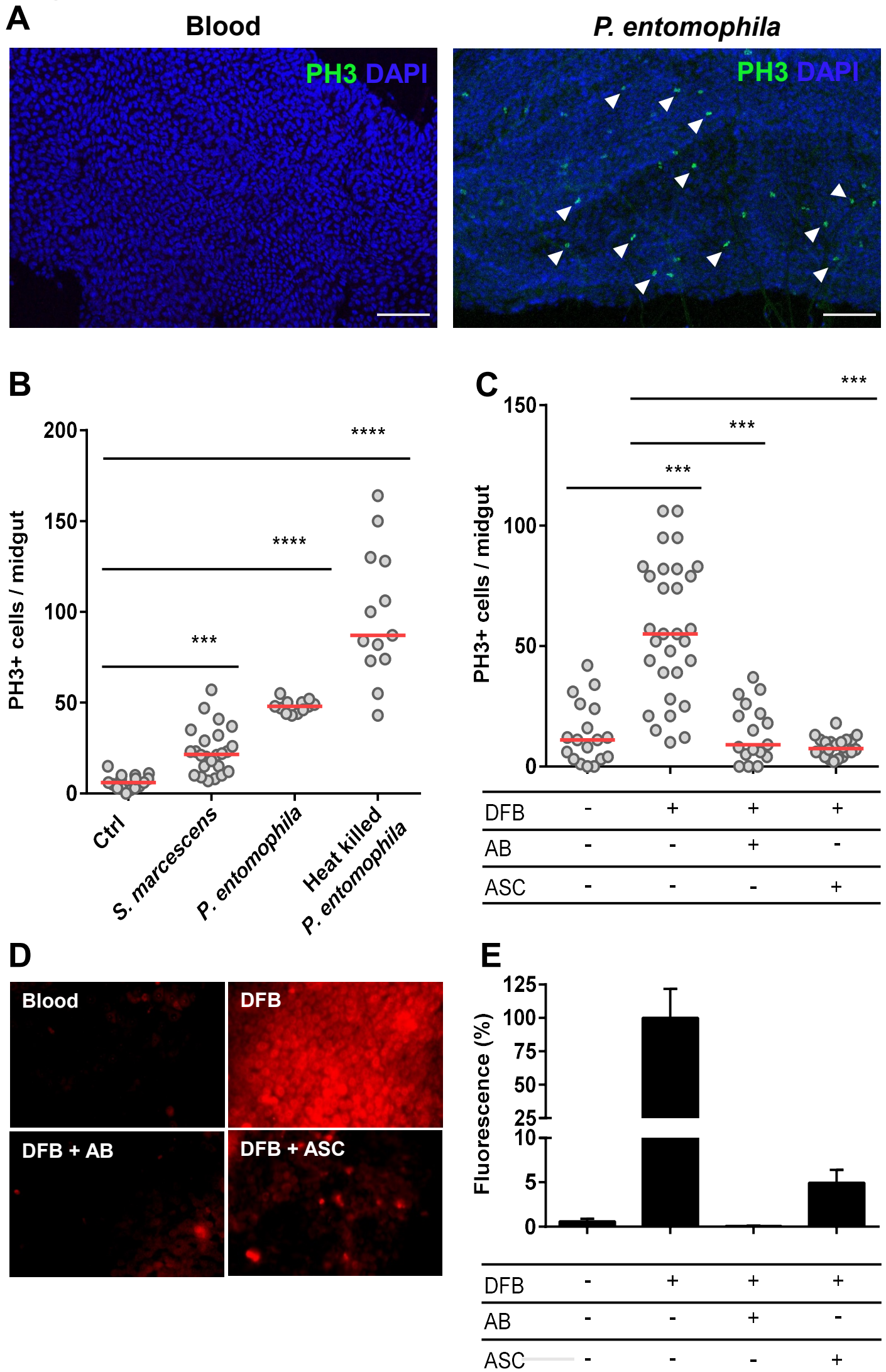
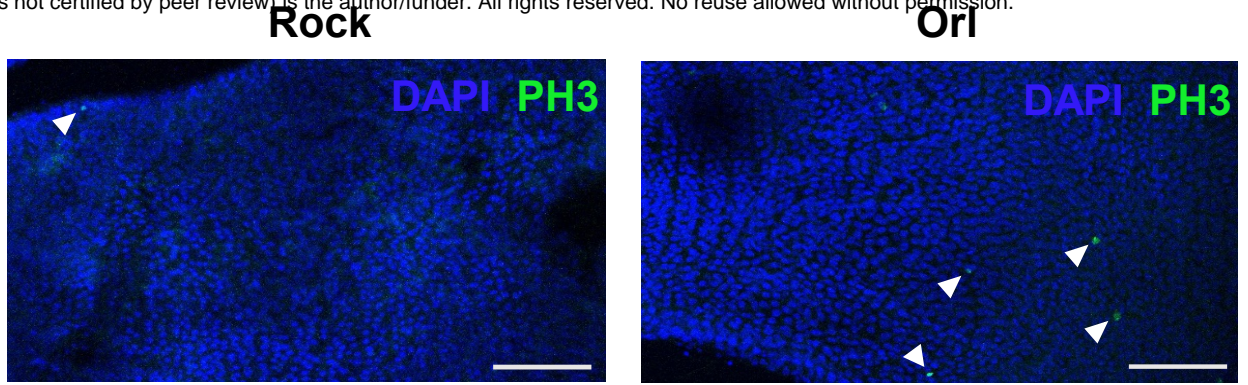
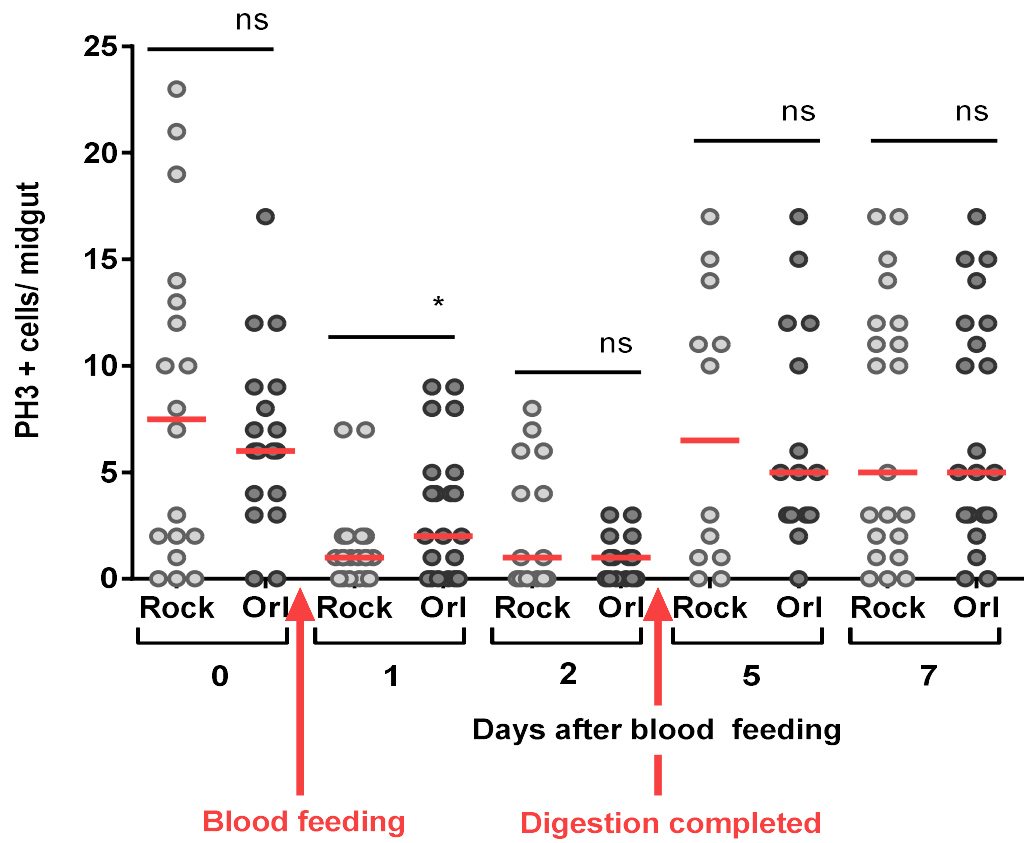


Figure 3

A



B



C

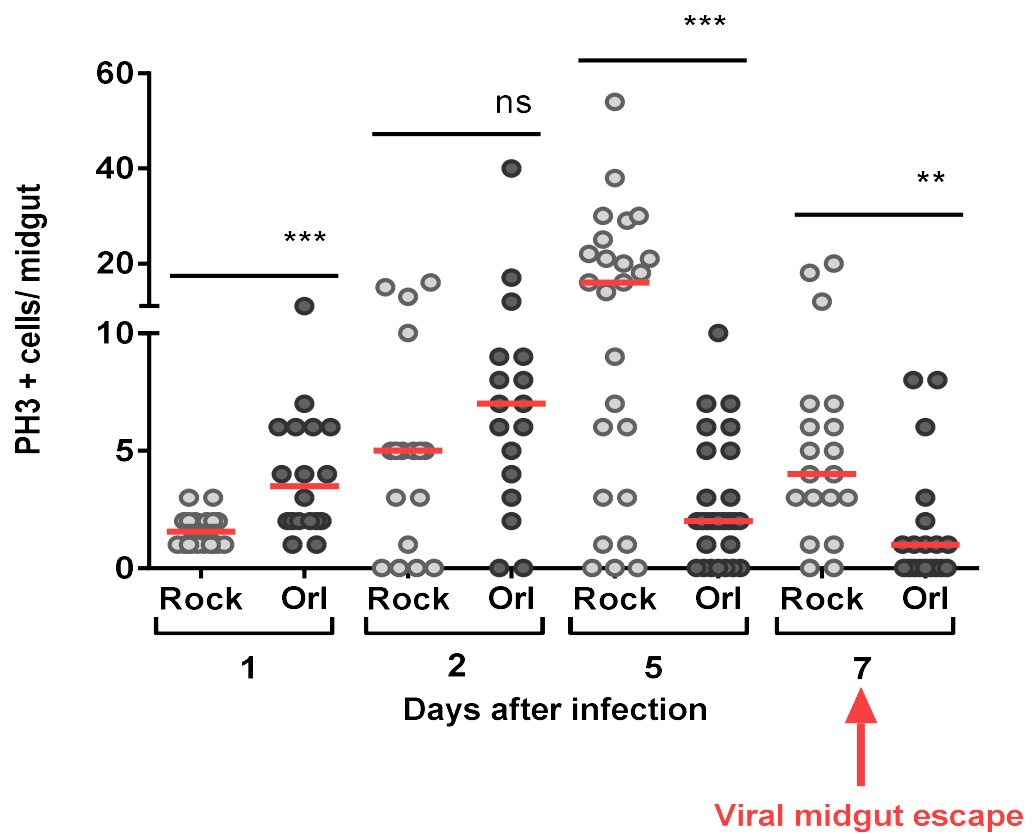
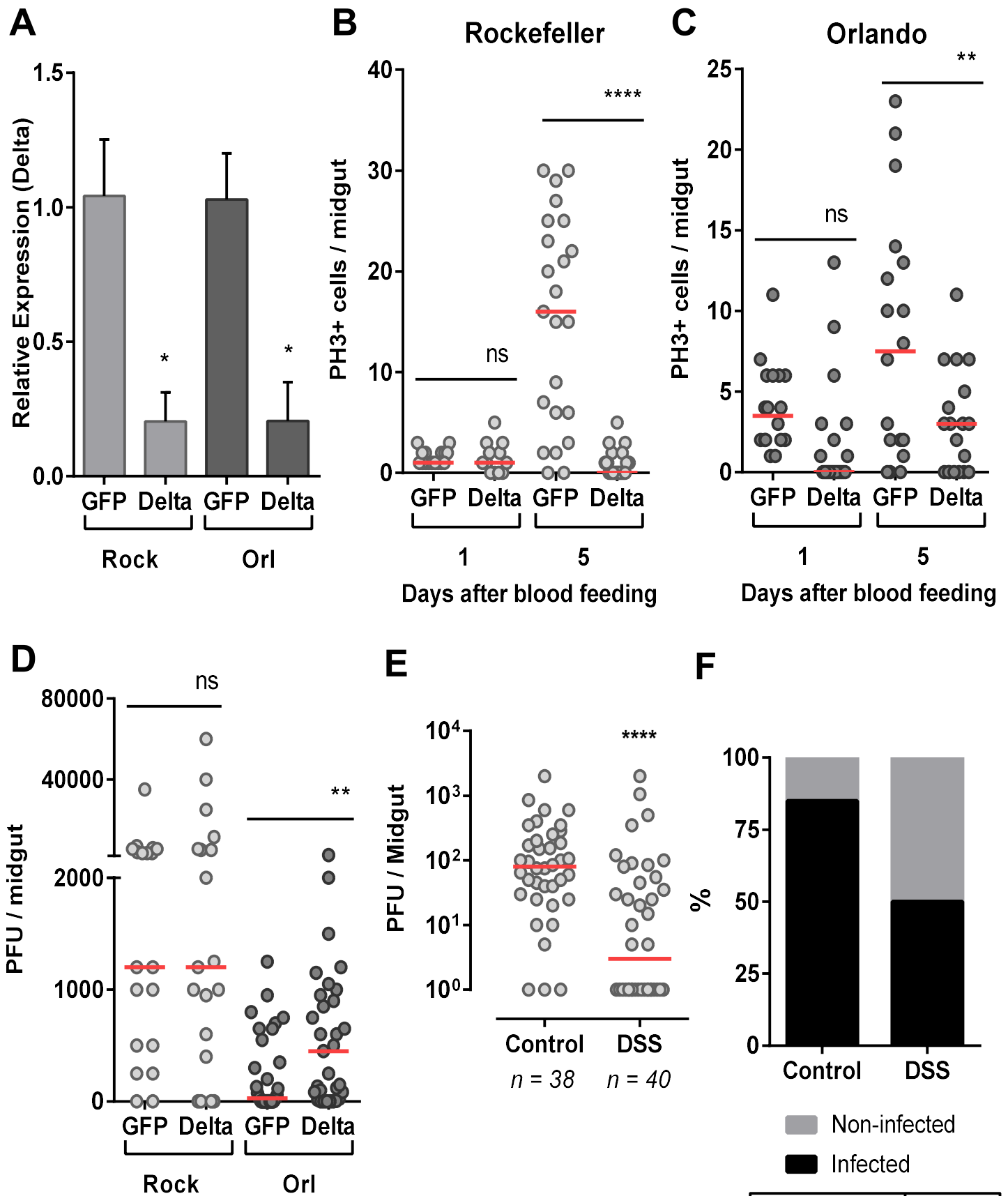


Figure 4



Chi-square	
Chi-square, df	27.92, 1
z	5.284
P value	< 0.0001